A seismic field test with a Low level Acoustic Combustion Source and Pseudo Noise codes

Bjørn Askeland [a *], Bent Ruud [b], Halvor Hobæk [a], Rolf Mjelde [b]

[a] *Department of Physics and Technology, Allégt. 55,University of Bergen, 5007 Bergen, Norway*
[b] *Department of Earth Science, Allégt. 41, University of Bergen, 5007 Bergen, Norway*

Abstract

The Low level Acoustic Combustion Source (LACS) is a new type of pulsed underwater acoustic source with an output level of 0.5-1.0 barm peak to peak. The source is based on a combustion engine and intended for shallow seismic surveys. It operates at 5 m depth and is able to fire pulses at a rate of up to 11 shots per second. Because of the source's low output level, it is expected to be more suitable than other sources in environmental sensitive areas. The low pulse level may be compensated for by an integration of energy from a sequence of pulses. This article describes the results of a seismic field test in Byfjorden outside Bergen, Norway. The best seismic result is achieved using deconvolution or an iterative correlation method where the correlator sequence is recorded right below the seismic source. Compared with airgun results along the same survey path, the seismic picture based on the LACS source gives a clearer presentation of the bottom layers.

Key words: Seismic source; marine source; time coding; correlation; seismic profiling ;pulsed seismics

1. Introduction

This paper presents a marine seismic source with a coding principle which is related to other different scientific disciplines such as radar, communications and ultrasound. Common for radar, ultrasound and seismics is the objective to measure distance to a target with good resolution.

In radar technology the range/resolution problem was originally solved by keeping the radar pulse short and the output level high. A longer range was achieved by an increase of the output level. During the 1950s a solution which used lower transmitter peak levels was found. The radar range was sustained by transmitting longer compressed radar pulses (Cook and Siebert, 1988). The long pulses provided high energy for the range requirement while the compression was necessary for the resolution.

Coded sequences similar to the compressed codes of radar can be found also in communication systems as direct sequence spread spectrum (Proakis and Salehi, 2002). While the

[*]Corresponding author. Tel +4755911681;fax: +4755589440.
E-mail address: bjorn.askeland@ift.uib.no

objective of military communication systems is to provide resistance against jamming, civilian systems use the codes to provide resistance against multipath propagation or to separate channels in a code division multiplexing system. One of the most common systems using direct sequence technology is the Global Positioning System (Freeman, 1994).

Coded sequences in ultrasound have been introduced in medicine during the last 5 years (Chiao and Hao, 2005). The objective is to use lower transmitter peak levels to obtain a good range and resolution.

Vibroseis is a well known chirped source which is used in land seismics (Baeten and Ziolkowski, 1990, Lindsey, 1991). A marine version of the Vibroseis also exist (Baeten and Ziolkowski, 1990). Swept pulsed sources can also be used (Park et al., 1996). The purpose of the sweep is to provide resolution while the continuous signal or a large number of pulses provide high energy. Pulsed sources do not have to sweep. The Mini-Sosie is an example of a handheld source which uses pseudorandom codes similar to the LACS code of this article.

In marine seismics airgun technology is the prevailing technology. A disadvantage of single airgun sources is bubble noise. A tuned array consisting of different volume airguns is a common remedy against this type of noise (Langhammer et al., 1995). For shallow penetration, an array is unnecessary and the bubble noise is undesirable. In such applications or in environmental areas, the bubble free low level LACS may be a competitor to airguns.

A suitable area for the seismic field test with the LACS was Byfjorden outside Bergen in western Norway. The objective of this test was to image shallow bottom sediments and compare the results with an airgun trial from 2004. Maps of the area indicate a sea depth between 154 and 373 m. The sediments of the area are glacial deposits, and the basement is crystalline rocks.

2. The LACS source

2.1. A pulsed combustion source

Figure 1 The LACS during deployment (1a) and the exhaust which is conducted to the surface in a tube (1b)

The LACS is an example of a pulsed seismic marine source which is easy to operate and is intended for shallow seismics in environmental sensitive areas. The source is shown in Figure 1a. The LACS is not the only source which profiles itself as environmental friendly. Also an electro-mechanical chirped marine vibrator made by Petroleum Geo-Services is intended for areas where use of airguns are considered to be inappropriate (Tenghamn et al., 2006). Also the Mini-SOSIE hand held vibrator for land seismics is described as environmental friendly (Driml et al., 2001).

The LACS principle is based on a one cylinder combustion engine which is positioned around 5 m below the surface. An acoustic pulse can be fired at specific times. Each pulse has lower output energy than airguns and is therefore more environmental friendly. It is driven by petrol and air which simplifies the operation. Although a compressor is still needed, the purpose is just to supply low pressure air to the combustion below the surface. As shown in Figure 1b the combustion gas is brought to the surface by a separate tube, so no gas is released in the sea, and accordingly the acoustic pulse is free of bubble noise. The 20 dB bandwidth is around 150Hz.

In order to compensate for a low output level, the seismic principle of the LACS is to use a high pulse rate. Being able to transmit up to 11 pulses per second, 110 transmitted pulses is the maximum during a 10 second interval.

2.2. Correlation

Correlation attenuates noise and integrates the energy of the pulses. How successful the correlation is, depends on the timing of a series of pulses which is the code of the sequence. In (Askeland et al., 2006) a proposed coding and decoding principal based on Pseudo Noise (PN) sequences is presented. The LACS is coded with randomly spaced pulses. Correlation is used to detect and separate the reflections. Note that a reflection is also a sequence of pulses. Note also that a weakness of systems using a correlation principle usually is a limited dynamic range caused by a non ideal autocorrelation function. If the bandwidth is limited or the code length is fixed, the autocorrelation function has sidelobes which hide the weaker reflector sequences. This problem is in telecommunications called a “near-far” field problem which means that a strong source near a receiver prevents weaker sequences from being detected (Majmundar et al., 2000). One of the objectives of the test was to see if the dynamic range of the coding was sufficient with the selected positions of the source and the streamer.

The dynamic range of a correlation code can in general be adjusted by bandwidth and sequence length. Since the LACS bandwidth is fixed, the easiest way to improve the correlation function is to increase the sequence length. Alternatively, a larger source or an array of larger sources must be used. Since survey time increases linearly with the integration time, the transmission length must be limited to a practical length. It is therefore natural to compare the sequence length with the time between each shot of airgun technology. The sequence of the coding of this field trial was therefore limited to ten seconds.

Another way of improving the correlation function is to optimize the code. The sequence can be synthesized in a large number of ways. If one pulse can start in one of 100 timeslots and there are 100 pulses in each sequence, there will be 100^{100} ways of synthesizing the sequence. Some of these autocorrelation functions have better correlation properties than others. Finding the most ideal sequence is an interesting field, but coding requires also an accurate source. One of the objectives of the tests was therefore also to obtain the statistical parameters related to the firing time.

Another objective of the test was to find the best principle of the correlation sequence of two alternative methods. Any correlation method requires a sequence which is correlated with the recorded data. In telecommunication systems, the correlator sequence is a deterministic signal which is present in the receiver. Received signals are expected to have a high correlation with

one of the sequences. This assumption works well for electronic circuits based on crystal accuracy, but is more difficult to obtain in acoustics with mechanical sources and larger time jitter. Even though the theory of correlation works well, there may be pitfalls during the practical implementation. One of the potential problems of the LACS is how the correlator sequence should be obtained. Two different methods are proposed: The first method is to use the logged sequence from the LACS hydrophone directly as a correlator sequence. This method is simple and very practical since the LACS hydrophone is a part of the LACS source system. A new correlator sequence is recorded for each new trace.

The second method is to synthesize a sequence based on a far field pulse recording. This method is suggested since it was uncertain prior to the test whether the recording of the LACS hydrophone would be representative for the signal leaving the source. Measuring the pulse at 80 m depth would guarantee that the pulse used in the correlator is representative for the pulse which actually leaves the source. The next step is to replace each pulse recorded by the LACS hydrophone with the far field signature. Since the LACS adds a stochastic time variable to the firing time, the firing times must be measured. The exact firing times of each sequence can be found by correlating the first pulse of the sequence with the rest of the sequence. The correlation peaks will show the firing positions and the energy level of the actual pulse. The correlator sequence is then finally constructed by a substitution of the far field pulse in the positions of the correlation peaks. Each individual pulse level is then adjusted according to the measured pressure level of each correlation peak.

3. Data acquisition

3.1. Acquisition system

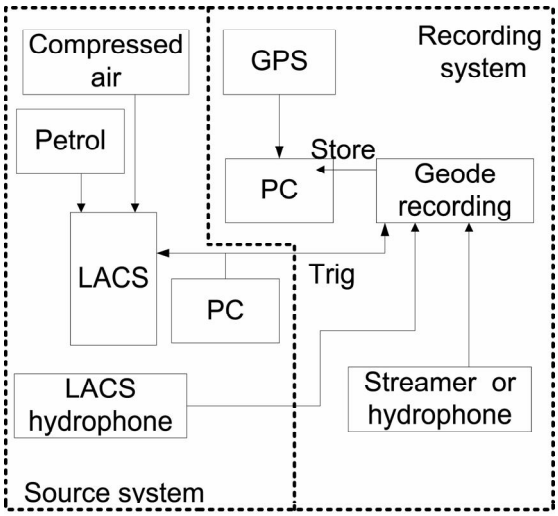

Figure 2 A block diagram of the acquisition system

A block diagram of the acquisition system consisting of a source system and a recording system can be seen in Figure 2. The LACS was driven by compressed air and petrol which was supplied from the surface. The source system PC triggered the firing of the source while the PC of the recording system stored the data from the Geometrics Geode seismic recorder and navigation data from the GPS. Samples were taken at a rate of 1000 samples/s with 24 bit resolution. A recording of the LACS hydrophone located 2 m below the LACS was always taken. The second input was either from a hydrophone or from a streamer depending of the objective of the recording.

3.2. Recording types

The data acquisition was split in three types: a far field pulse signature recording, a streamer recording of a 3 km path and finally a recording of system noise without the source.

3.2.1. Far field pulse signature recording

As shown in Figure 3, the far field signature was measured with the vessel at rest and the far field hydrophone at around 80 m depth. The recorded far field pulse can be seen in Figure 4.

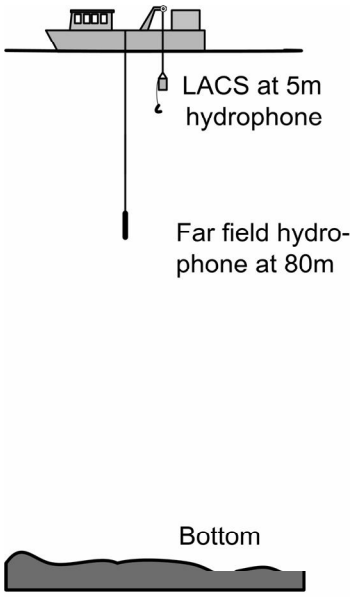

Figure 3 Far field pulse signature recording with the vessel at rest and a far field hydrophone at 80m.

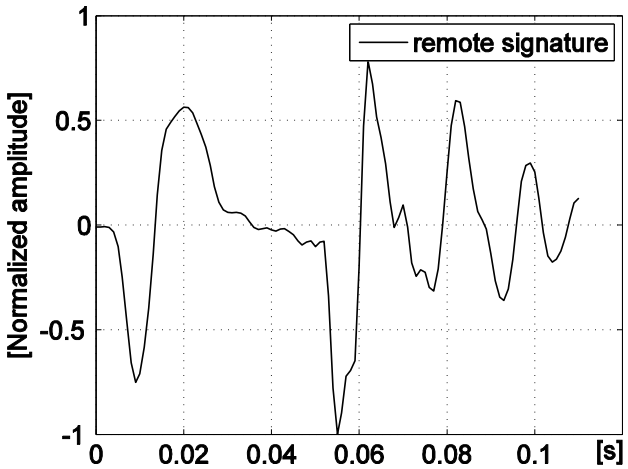

Figure 4 Far field signature recorded by a hydrophone at 80 m depth. This pulse was used as a building block for the synthesized correlator sequence.

3.2.2. Streamer recording

After the far field measurement was completed, the far field hydrophone was replaced by a streamer as shown in Figure 5.

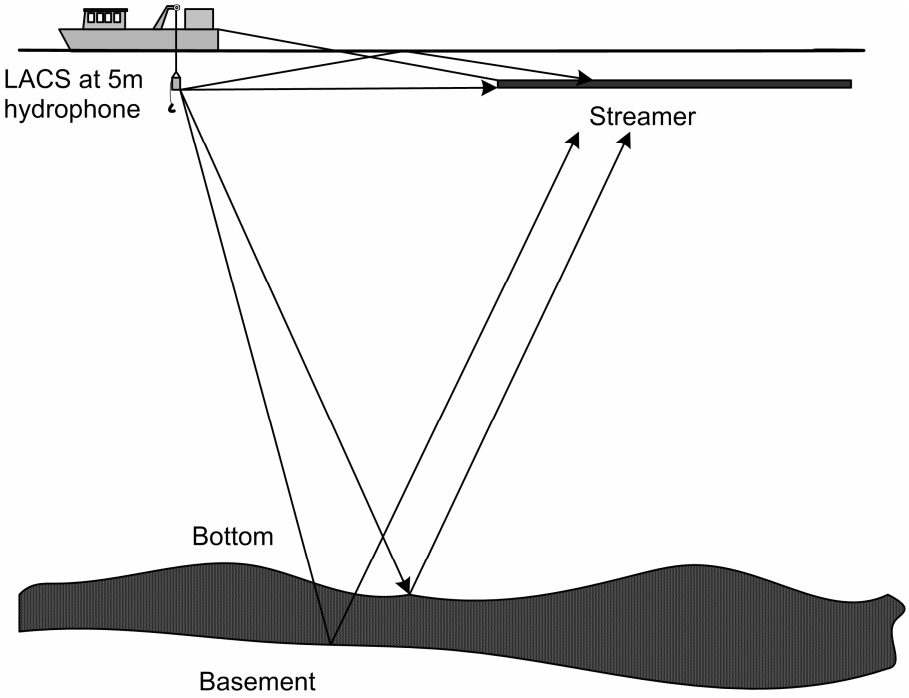

Figure 5 Streamer recording and indication of some of the most dominating reflectors

A sequence of duration 10 seconds consisting of 43 pulses was fired every 16 second along the line. Each recording had a duration of 12 seconds. Logged channels were the LACS hydrophone and the streamer. 4 seconds were necessary in order to transfer logged data from the logging system to the PC hard drive. The vessel speed was approximately 2.8 knots which corresponds to an average distance between each new sequence of 23 m. The distance to the streamer was 60 m. The streamer channel consisted of 21 hydrophones with individual distance 0.51 m. A sequence number was assigned to each logged sequence. The path started with sequence number SP1288 and ended with sequence number SP1440.

3.2.3. Noise measurement

After the path was completed, the system and background noise was recorded. During this test the LACS was turned off.

4. Data analysis

4.1. Deconvolution and correlation

In order to find the impulse response from seismic recordings, deconvolution is the typical approach (Robinson and Treitel, 1980). The impulse response of the channel can also be found using crosscorrelation (Haykin, 1978). The data analysis starts with correlation. Two different correlation sequences are used and compared. Next an iterative correlation principle is presented. This technique removes the blurriness which is present in the single correlation seismic image.

Finally, a deconvolved seismic image is presented and compared with the iterative correlation result.

4.2. Correlation

4.2.1. Single correlation with LACS hydrophone recording

x(t) is the signal from the LACS. In order to illustrate the sequence, an example of x(t) as a logged sequence by the LACS hydrophone is shown in Figure 6a. Its autocorrelation function is shown in Figure 6b.

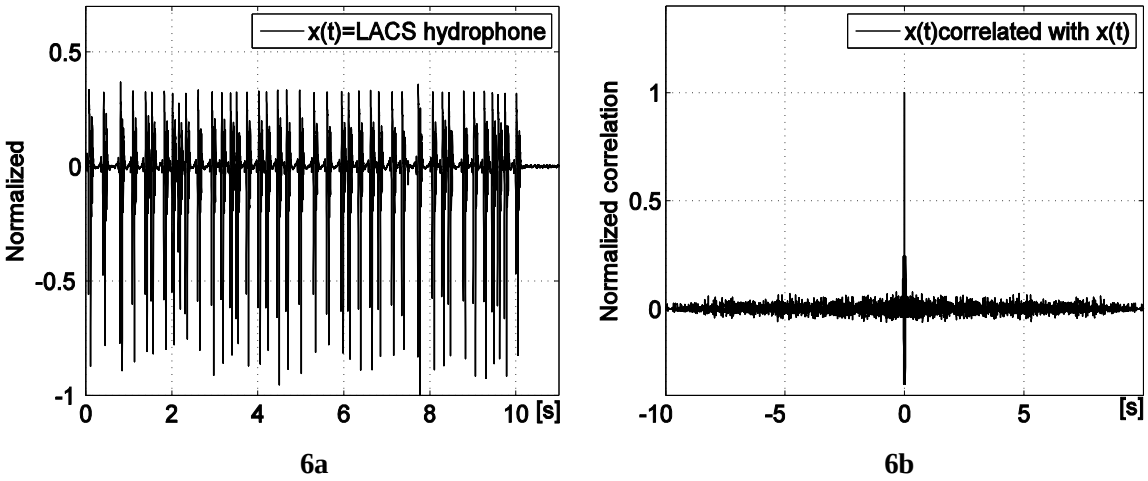

Figure 6 One of the LACS hydrophone recordings (6a) from the streamer survey and its computed autocorrelation function (6b).

It is assumed that data logged by the streamer is a sum of scaled and delayed versions of the transmitted signal x(t). Then the logged data of the streamer can be expressed as $y(t) = a_1 x(t-\tau_1) + a_2 x(t-\tau_2) + ..$ A physical interpretation is that a_i is the product of the geometrical spreading and the reflection coefficient while τ_i is the two way travel time (TWT) to the reflector. When x(t) is correlated with y(t), correlation peaks will occur where there is zero delay between the correlation sequence and the delayed version of x(t).

Figure 7 shows the recording of the first transmitted sequence of the path, SP1288. $h(t)$ is the channel between the transmitter and the streamer. The logged recording by the streamer = $y(t) = x(t) * h(t)$ where $*$ is the convolution operator. Delayed versions of x(t) can be found from the logging by correlating x(t) with y(t). The result of the correlation is shown for SP1288 in Figure 8a. Three distinct positive and negative correlation peaks can be seen in the figure. They represent the direct arrival, the bottom/basement reflection and the first multiple reflection. In order to obtain a timing reference of the correlation, the autocorrelation of Figure 6b is used. Since the recording of the LACS hydrophone is synchronized with the recording of the streamer, the peak of the autocorrelation function of x(t) represents t=0. Figure 8b shows the value of the crosscorrelation function within the first 1500 ms two way travel time.

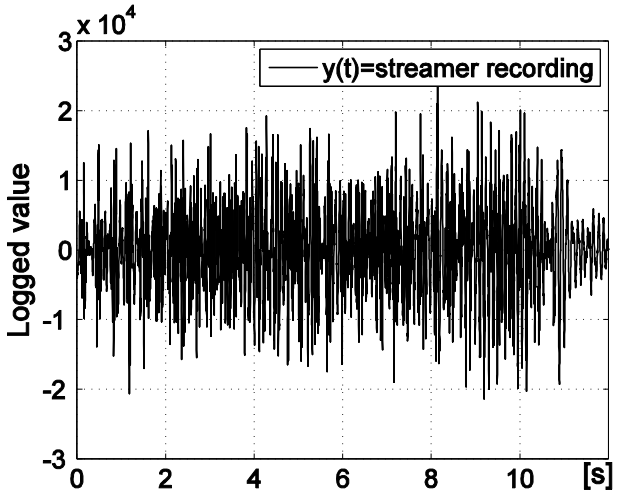

Figure 7 One of the streamer recordings y(t) of the streamer survey.

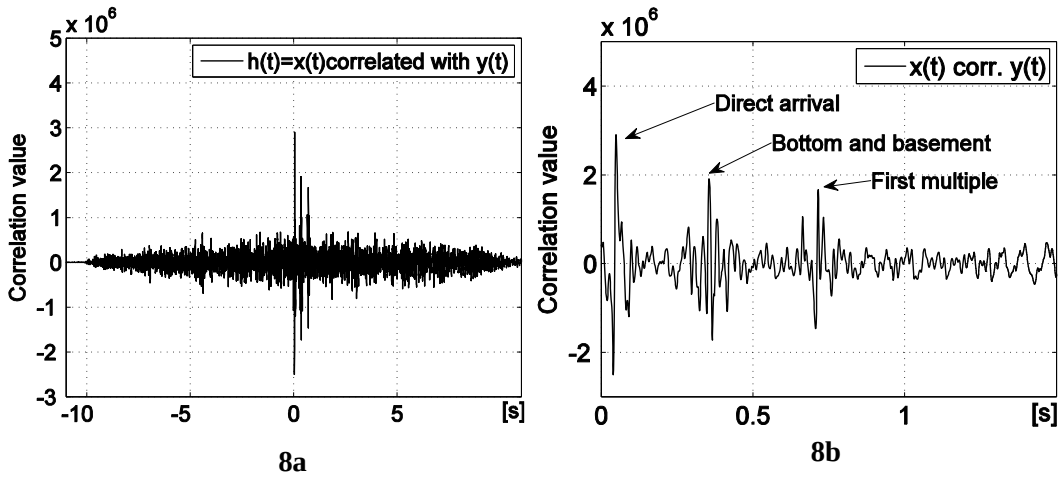

Figure 8 LACS hydrophone recording x(t) correlated with the streamer recording y(t). Figure 8b is a zoomed version of 8a.

The processed result of Figure 8b is entered into a matrix as a trace column for each sequence along the path. In total the path consisted of 152 traces . When the matrix is plotted, a picture is created as shown in Figure 9a. The direct arrival and sea surface reflections can be seen around 50 ms, the bottom layers can be seen in the middle of the picture and a weak first multiple can be seen further down. Figure 9b shows Figure 9a zoomed to the bottom layers between 0.3 to 0.7s TWT. The bottom layers are blurry, partly caused by the sea surface reflection which can be removed using the sign of the calculated correlation. Figure 9c shows the seismic image when h(t)>0. Even if the image now should be clearer, it is still blurry.

Fig 9a,9b and 9c

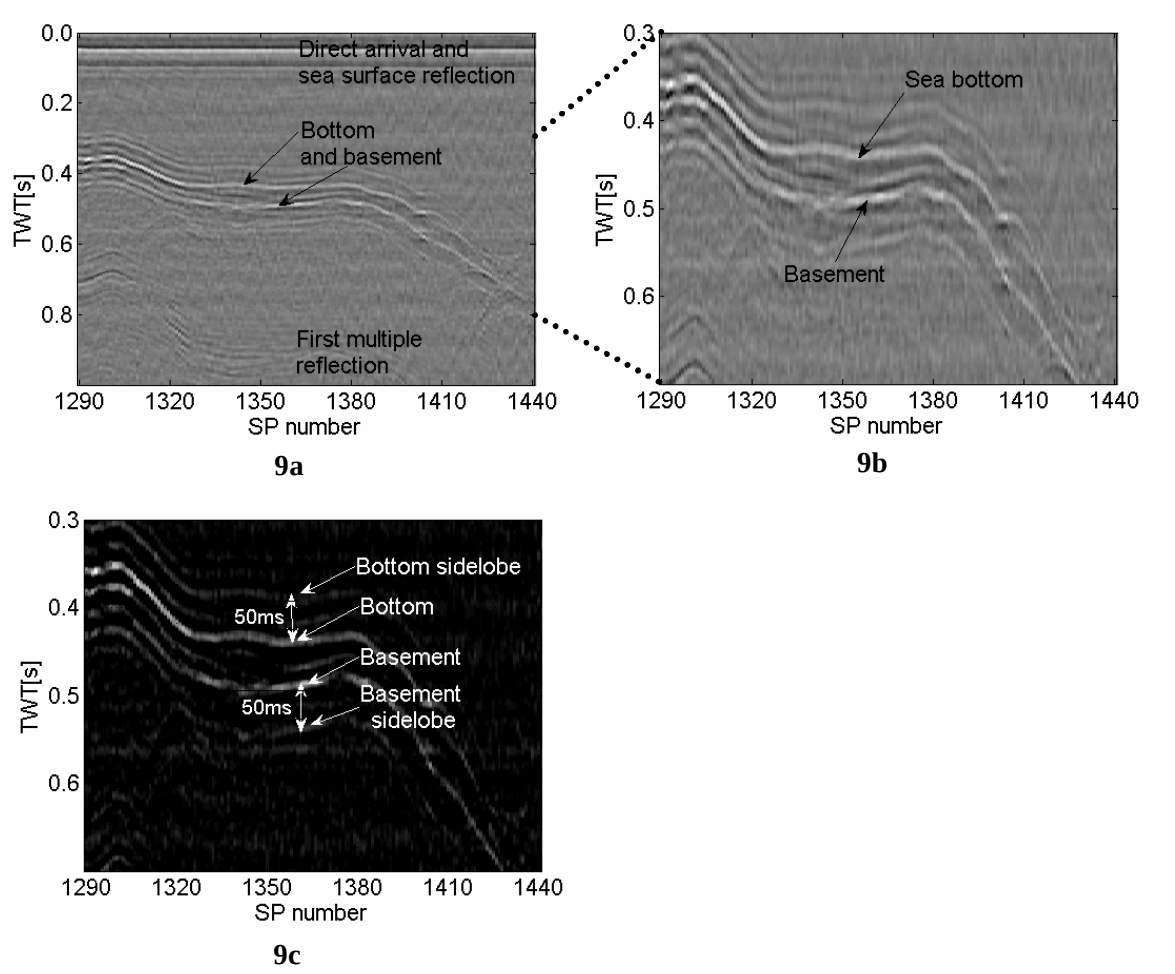

Figure 9 Raw correlation image based on the LACS hydrophone data and the streamer data.

4.2.2. Single correlation with field synthesized correlation sequence

One of the objectives of the field test was to correlate with a synthesized sequence based on a far field signature. The image based on the synthesized sequence is shown in Figure 10. The image is slightly more unclear than the image of Figure 9b. The difference is not large, but it is convenient that the most practical method gives the best result. The parallel lines must be caused by a variation of the pulse signature. Based on this comparison it is clear that using the LACS hydrophone directly as a correlation sequence is the best choice. The LACS hydrophone provides the best seismic image and is also more practical since a remote signature measurement will not be necessary prior to the survey.

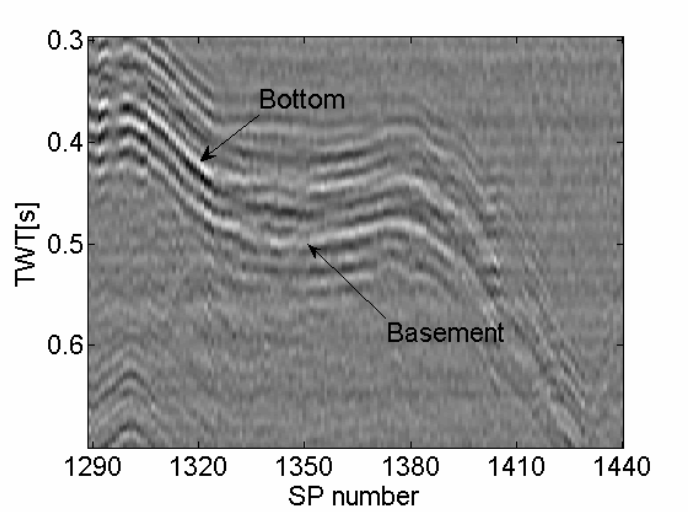

Figure 10 Correlation image based on the far field synthesized sequence and the streamer data.

4.2.3. Improvement of the seismic image by iterative correlation

The blurriness of the images can be removed with iterative correlation. The parallel traces of the image are partly caused by the sidelobes of the autocorrelation function. As seen in Figure 11, the autocorrelation function has several negative and positive sidelobes within the pulse interval. For the selected sequence, the largest positive sidelobes are up to 23% of the main peak and occur at ±50ms. Therefore the positive value of h(t) will present the bottom and basement as strong reflectors, while there will be weaker correlation peaks of distance ±50ms from the main peak.

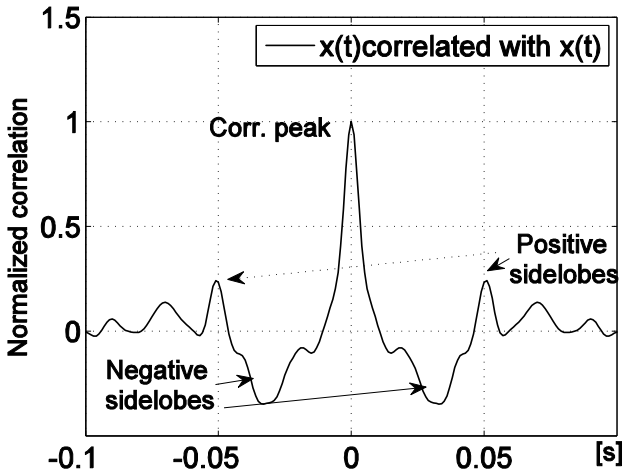

Figure 11 Zoomed autocorrelation function of a LACS sequence. The sidelobes cause blurriness of the seismic images.

An iterative correlation method has been used to improve the seismic image of Figure 9b further. The dynamic range where sequence levels can be detected, is limited by the level of the strongest received sequence and the sidelobe level of the autocorrelation function. For the sequences of this field test, the sidelobe level is around 0.23 times the peak value for delays within the pulse width and 0.1 for delays larger than the pulse width. Sequences with a relative level less than the sidelobe level will remain embedded in sidelobe "noise".

Instead of increasing the dynamic range by increasing the sequence length, the dynamic range can be expanded indirectly in an iterative process. The idea is to remove the most powerful sequence from the logging, then repeat the correlation until only uncorrelated noise remains. A flow diagram of the routine can be seen in Figure 12. For each new correlation, the largest corresponding time sequence is removed from the logging. Then the correlation is repeated with the reminder of the logged sequence. The largest sidelobes also disappear with the subtraction. A consequence of the subtraction is an ability to detect sequences, which are spaced by less than a one pulse width, with good resolution.

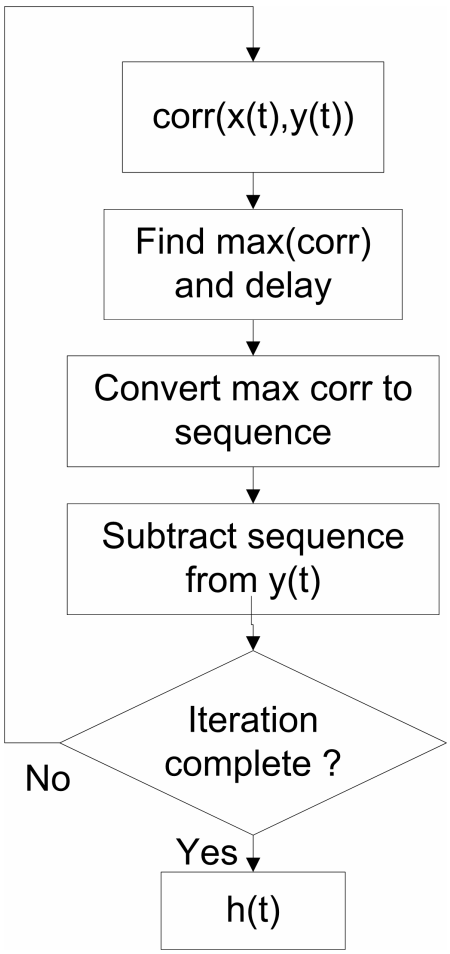

Figure 12 A flow diagram of the iterative correlation method where sequences are subtracted from the logged data between each new correlation. The process removed sidelobe noise from the seismic image.

Since the dynamic range is related to the energy of the highest correlation peak, the upper part of the dynamic range will be adjusted to the second largest peak for each new correlation. For each time the remaining largest correlation peak has less energy than the previously subtracted, the dynamic range moves towards the weaker signal levels. After a certain number of subtractions, only uncorrelated noise remains. Figure 13 shows how the correlation peaks are removed with an increasing number of iterations. The green curve is the original crosscorrelation while the red curve is the new crosscorrelation after the corresponding time sequence has been subtracted from the recording.

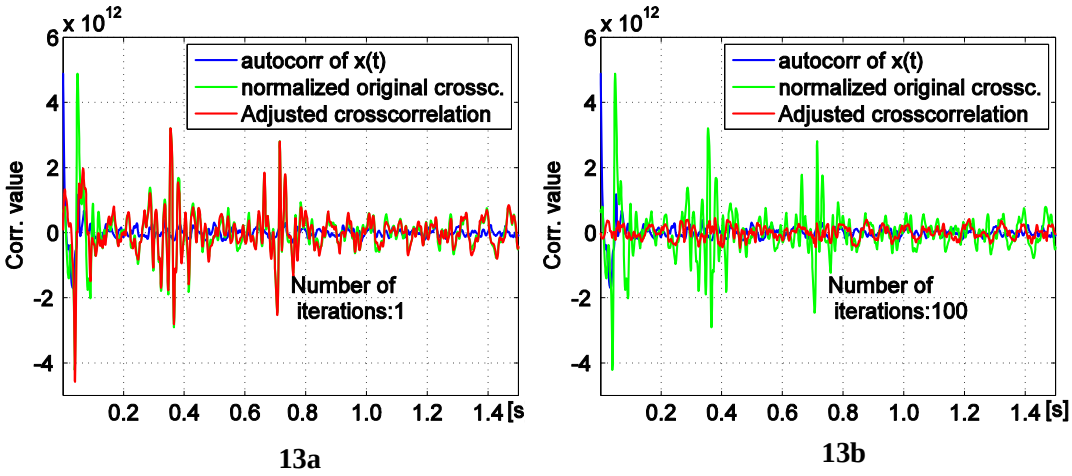

Figure 13 Iterative correlation. The red line indicates the crosscorrelation result after a certain number of correlated and subtracted sequences. The green line is the result after one single crosscorrelation. Figure 13b shows the result of the crosscorrelation after 100 iterations. At this stage only uncorrelated noise remains.

Mathematically the logged signal can be expressed as a sum of the outgoing sequences as: $y(t) = \sum_{m=1}^{M} a_m x(t - t_m) + n(t)$ where x(t) is the signal recorded 2 m below the source. $n(t)$ is the uncorrelated noise of the recording. If n(t) is neglected the equation is simplified to: $y(t) = x(t) * h(t)$ which means that $h(t) = \sum_{m=1}^{M} a_m \delta(t - t_m)$. As presented in Figure 14, the channel is now a sum of delta functions which more clearly shows the position of the reflections.

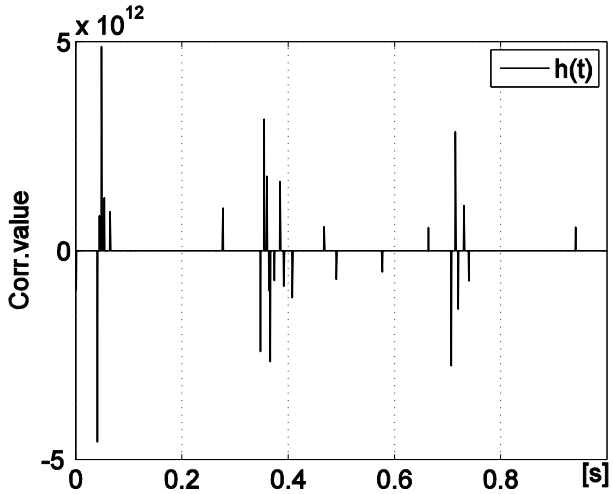

Figure 14 A result of the iterative correlation is a channel impulse response h(t) described as a sum of delta functions.

A new attempt to remove surface reflections is done by selecting h(t)>0. If each trace of $h(t)$ >0 then is entered into a new matrix, the matrix can be plotted as a seismic image as shown in Figure 15.

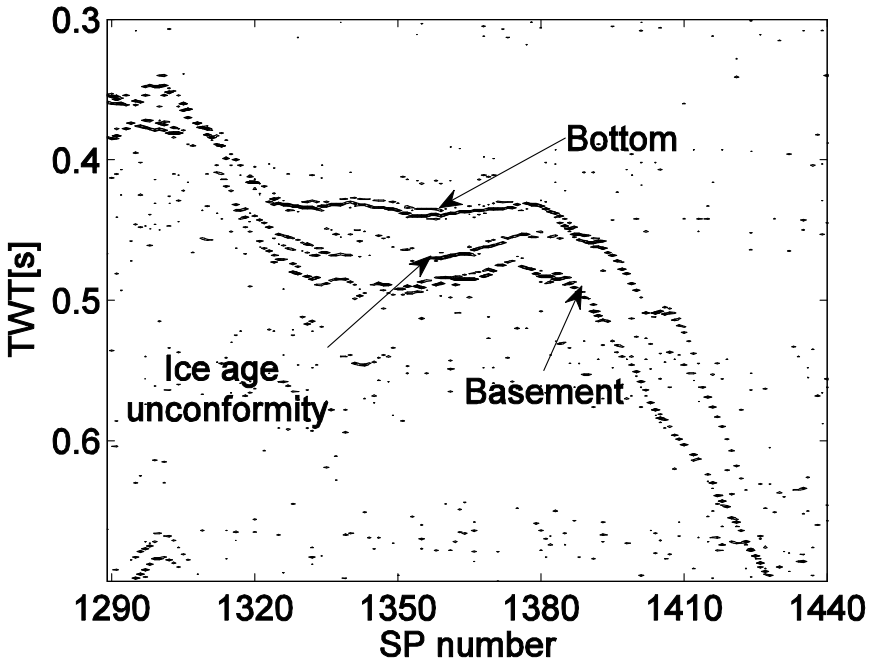

Figure 15 An image plot of Byfjorden based on the iterative correlation method with h(t)>0. Taking the sign of the impulse response of the channel removes the sea surface reflections.

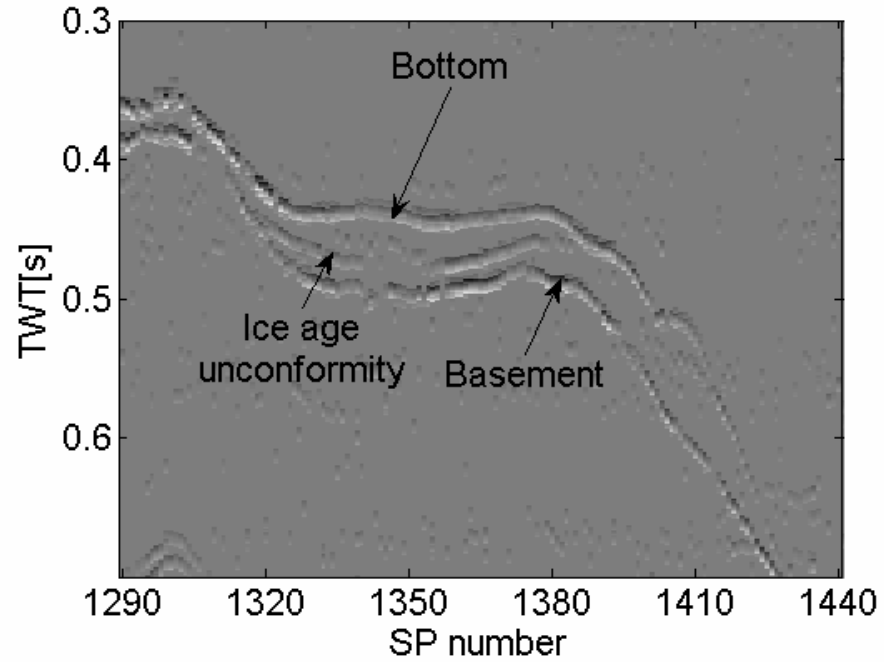

Figure 16 A cosmetic presentation of Figure 15. The delta functions of the positive part of the impulse response have been convolved with a single period sine pulse of duration 10ms.

White background is used for contrast purpose and only the interesting area from 0.3s-0.7s TWT is shown. The image is no longer blurry, but has two or three distinct lines. The upper line is the bottom while the lower line is basement. The middle line is interpreted as sediments from an erosional unconformity related to a glacier re-advance at the end of the last ice age, about 13 000 years ago (Mangerud et al., 1995).

Geophysicists are not used to the presentation type of Figure 15. In order to provide more similarity to common seismic images, the impulse response has been convolved with a single sine pulse of one period equal to 10 ms. This will be analogue to a clean airgun pulse of 10 ms duration. A result of the convolution is shown in Figure 16.

4.3. Deconvolution

Deterministic deconvolution in the frequency domain was applied to the LACS recordings in Seismic Unix. Denoting the LACS hydrophone data as $X(\omega)$ and the streamer data as $Y(\omega)$, the transfer function $H(\omega)$, i.e., the seismic response, was computed as :

$H(\omega) = X(\omega)^* Y(\omega)/(X(\omega)X(\omega)^* + \xi)$. $X(\omega)^*$ is the complex conjugate of $X(\omega)$. ξ is a stabilizing factor which was set to 0.0001 E where E is the total energy of x(t).

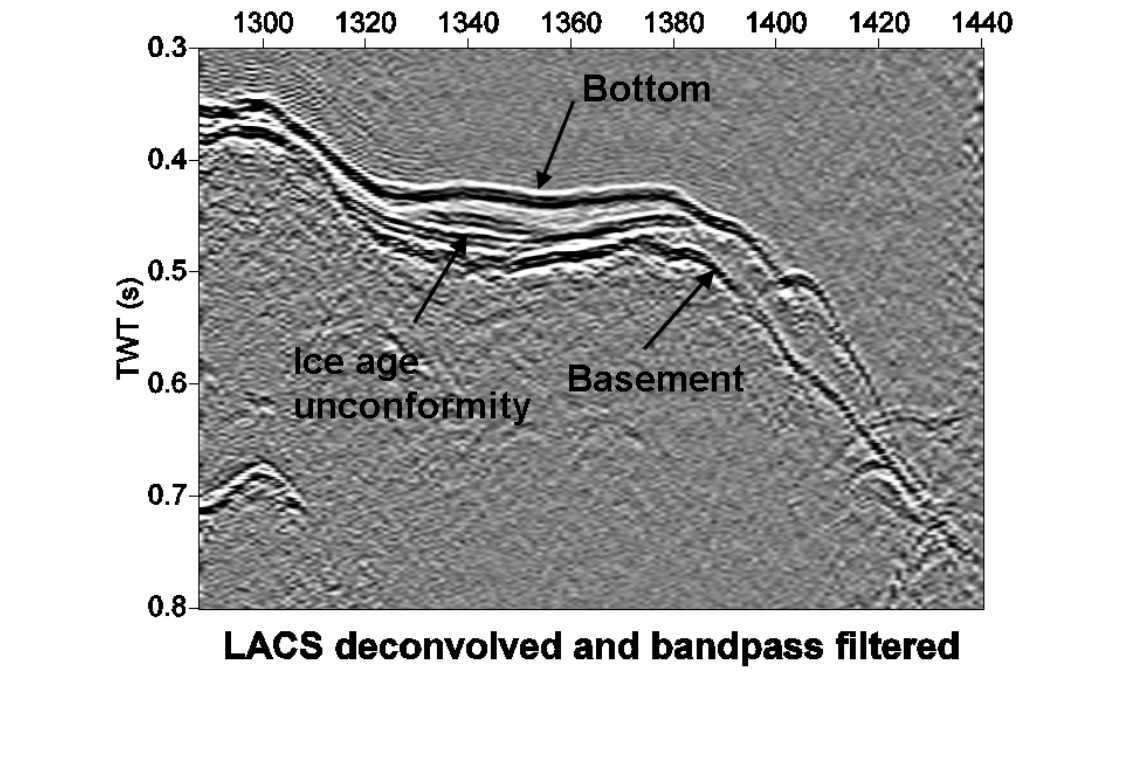

Figure 17 An image plot of Byfjorden based on a Seismic Unix deconvolution routine.

A seismic image based on deconvolution is shown in Figure 17. The image presents a strong sea bottom and basement reflection. Also internal layers can be seen. The deconvolved image has great resemblance to the image based on iterative correlation.

4.4. Noise measurement and uncorrelated noise

Shortly after the path was completed system and background noise was recorded. During this recording the LACS was shut off. As shown in Figure 18a, the noise is dominated by frequencies between 5 and 20 Hz. Figure 18b shows the frequency contents of the reminder of the streamer recording after a completion of the iterative correlation subtraction. It is interesting to see that the reminder of x(t) has almost the same frequency contents as the noise measurement of SP1969.

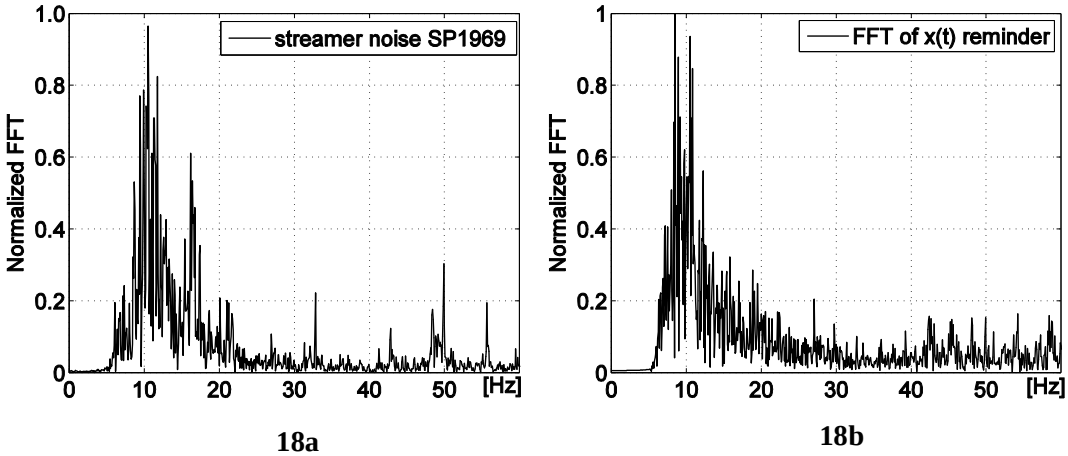

Figure 18 FFT of the system noise recording with the LACS shut off (18a). The FFT of the reminder of the streamer recording after 100 iterations (18b)

4.5. Calculation of the source firing accuracy

The accuracy of the source is of great importance when it comes to coding theory. It does not make any sense to design codes with good correlation properties unless the codes can be fired accurately. Therefore the stochastic timing variable of the source and ignition system has been calculated based on all the pulses of the survey path. The individual distance between the pulses is known from the code. The actual firing times of a sequence can be found from the logged LACS hydrophone. The standard deviation of the difference between the actual firing time and the planned firing time calculated over all pulses of the path was 6.2 ms. This is higher than expected, but can possibly be reduced some by proper adjustments of the LACS ignition system. The actual firing time was found by correlating the first pulse of the sequence with the entire sequence.

5. Data from other field tests

5.1. Airgun data from 2004

A profile close to the LACS profile (see the map in Figure 20) was shot by a single airgun (Bolt Par 1900) at a depth of 5 m. The airgun has a 20 dB bandwidth larger than 500 Hz, but most of the energy is below 300Hz.

As seen from Figure 19a, the true seismic response of the sea bottom is hidden in a long series of rather strong bubble pulses. Also after a bandpass filter (15-300 Hz) the bubble pulses distort the seismic image as seen in Figure 19b. In this image, some bad traces have been removed and the time window has been focused on the sea bottom and the reflectors in the upper sea bottom sediments.

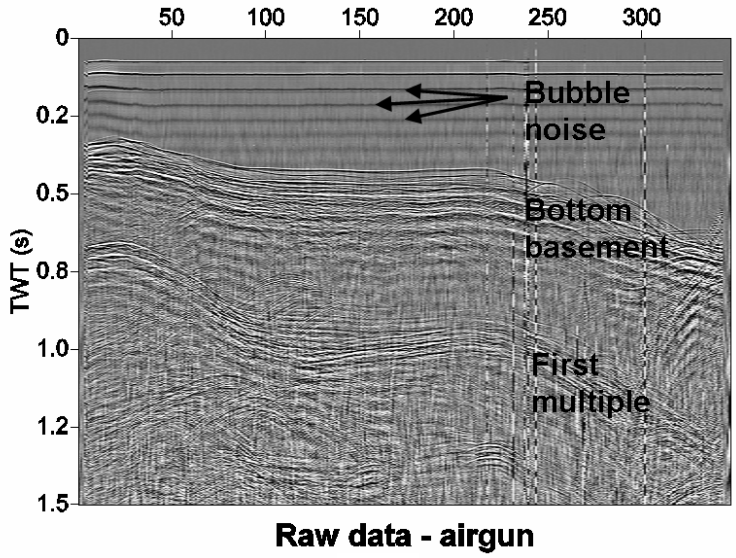

Raw data - airgun

19a

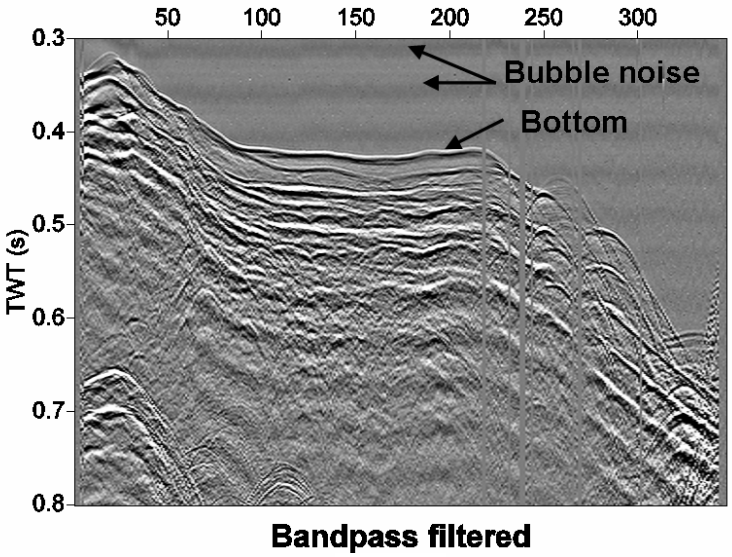

Bandpass filtered

19b

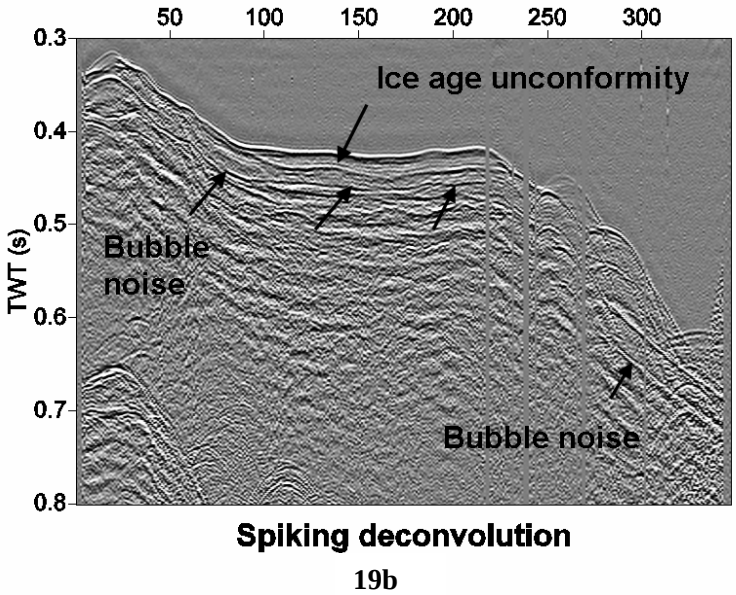

Figure 19 Airgun images of the path. Raw data (19a), band pass filtered (19b) and spiking deconvolution (19c). The images are less representative of the sediments than the LAC images of Figure 15 and Figure 17.

Since there was no near field recording of the signal generated by the airgun, deterministic deconvolution (as done with the LACS source) could not be applied, and we could only do statistical, spiking deconvolution. The time window used to compute the autocorrelation was set to 0.3-0.8 s. The filter length was set to 0.2 s, and prediction distance was set to 6 ms. The result of this spiking deconvolution is shown in Figure 19c.

Although this result is a significant improvement, the strong bubble pulses have not been completely removed. For instance, the first bubble pulse, about 40 ms after the sea bottom reflection, can still be seen.

The paths of the LACS field trial of 2006 and the airgun path of the 2004 field test can be seen in Figure 20. The LACS line has red dots while the airgun line is green.

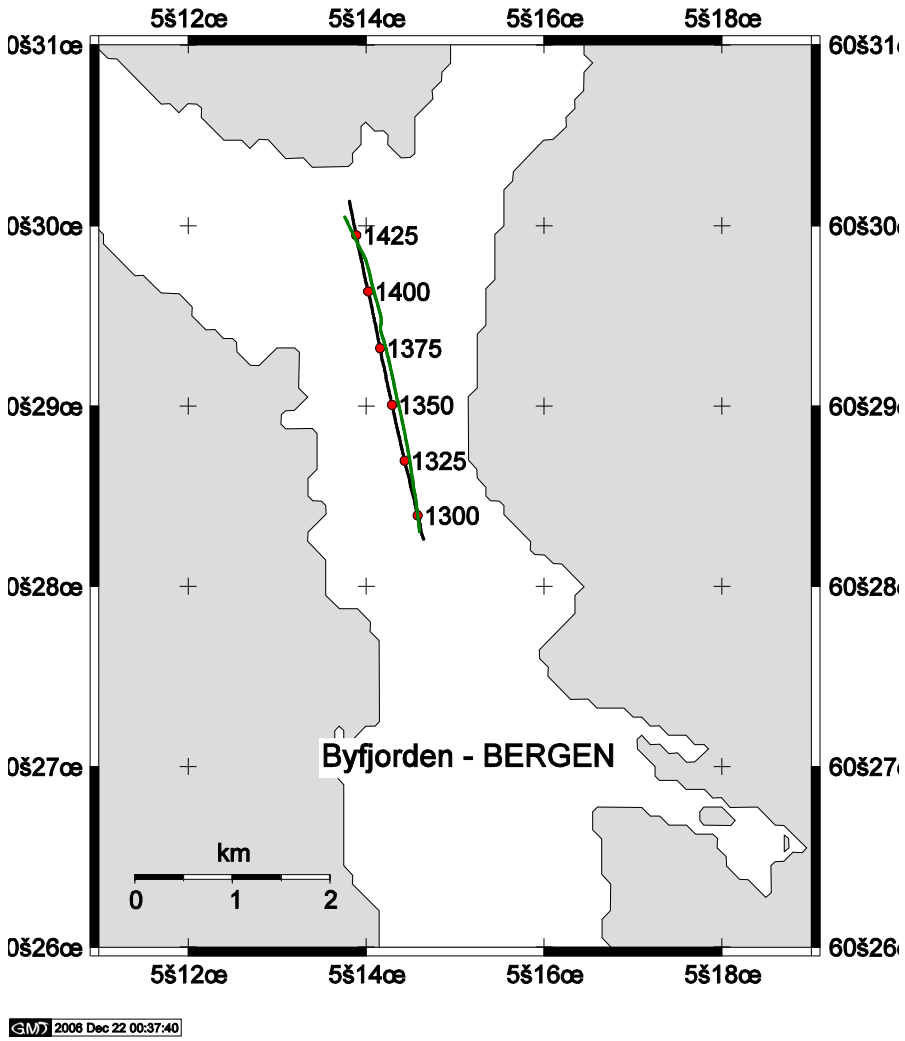

Figure 20 The LACS Streamer path of the field test is indicated the black line with red dots. The line recorded with airgun from 2004 is in indicated with green.

5.2. High resolution data with Topas from 2006

A high resolution image of a profile west of the LACS profile is shown in the upper part Figure 21. A Topas PS18 sub bottom profiler, which according to the manufacturer has a resolution of < 30 cm, has been used to create the image. Similarities of the profiles between the LACS deconvolved image, in the lower part of Figure 21, and the Topas image are indicated with lines. The ice age unconformity can be seen clearly in the Topas image while the penetration is too short to show the crystalline basement. A suggested basement has been indicated in the Topas image.

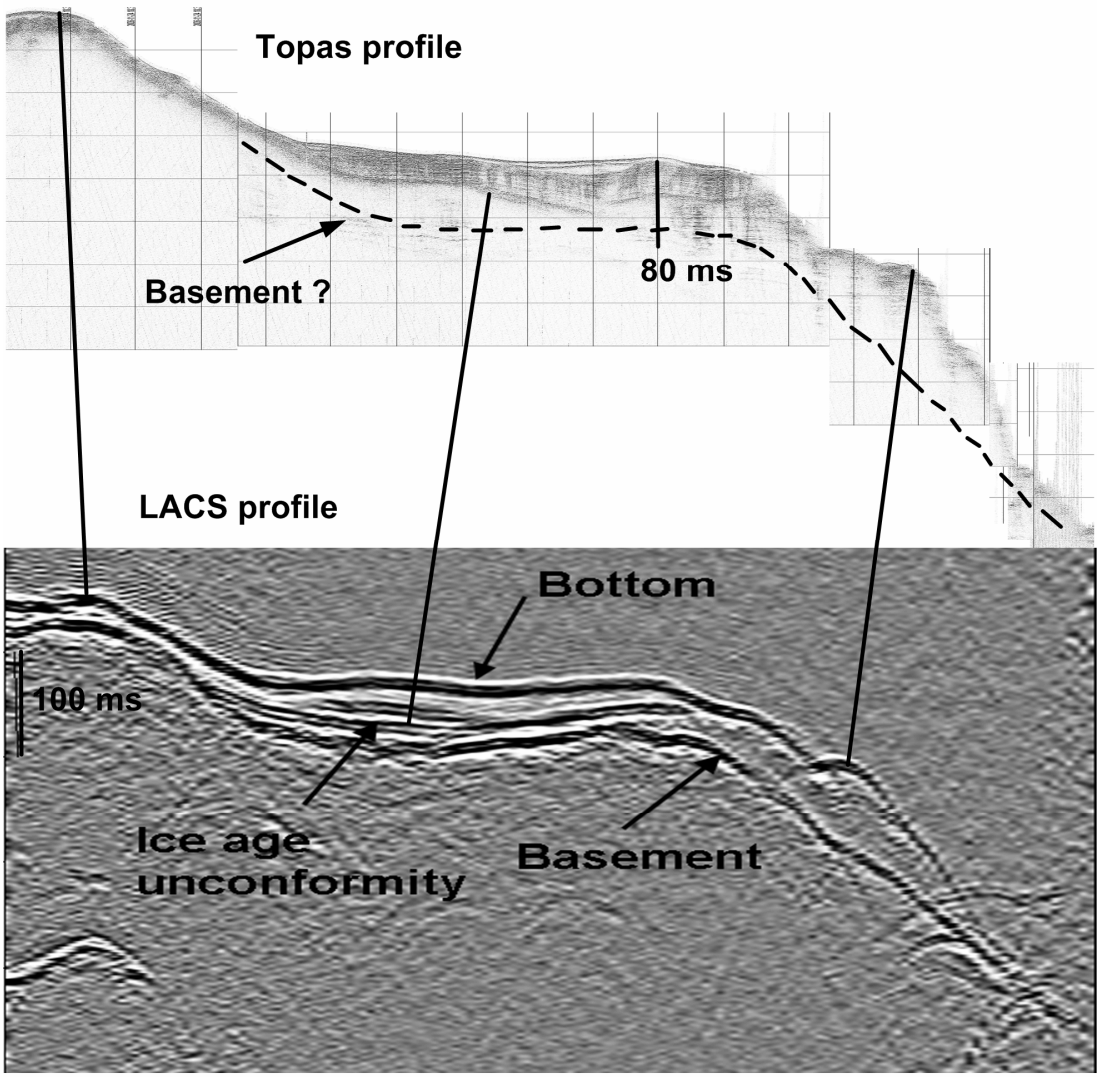

Figure 21 A high resolution Topas image confirms the ice age unconformity of the deconvolved LACS image.

6. Discussion and conclusions

The Low level Acoustic Combustion Source has successfully been tested as a seismic source on shallow ice age sediments in Byfjorden outside Bergen.

One of the objectives of the field test was to see whether the correlation principle would work. A potential hazard was a near-far problem where a dominating direct arrival embeds weaker reflectors in sidelobe correlator noise. A strong direct arrival was observed, but did not represent a problem with respect to the dynamic range.

Of the two possible correlation sequences, a recording of the LACS hydrophone worked better than a correlation sequence based on a measured remote LACS signature. This is convenient since a recording of a remote signature prior to the seismic survey is not necessary.

When the recording of the LACS hydrophone was correlated with the streamer recording for all the 152 sequences along the survey path, the result was a blurry seismic image. Two stronger

correlation traces representing the bottom profile and the basement can be seen, but parallel curves representing sidelobe noise and surface reflected noise disturb the image.

An iterating correlation principle can be used to further improve the image. The method correlates and subtracts one corresponding sequence from the streamer recording sequentially. Unwanted sidelobes disappear with each subtraction and an impulse response consisting of delta functions is created. When the positive part of the impulse response is presented as an image, surface reflections are removed. Figure 16 shows the impulse response after a convolution with an imagined clean sine wave of 10 ms period. This presentation type has resemblance to seismic images. Since surface reflections and sidelobe noise are reduced, the processed picture shows clearly the bottom, an ice age unconformity in the middle and the crystalline basement.

The deconvolved LACS image gives approximately the same information as the LACS image based on iterative correlation. A difference is that the contrasts are more dominating in the deconvolved image.

Except from the bottom profile, the rest of the airgun image of

c is different from the LACS results. The LACS gives a better image of the basement and probably a more reliable image of the interfaces between the sea floor and basement.

The firing time jitter of 6.2 ms is larger than expected. As an example of a more accurate source, airguns can be tuned to ±0.5 ms (Ziolkowski and Johnston, 1997). Despite this inaccuracy the method seems to work well.

Shallow seismics can also be done by other sources such as sonar, boomer, plasmagun, sparker and watergun (Verbeek and McGee, 1995). It remains to se in exactly which application the LACS has its greatest potential. Most likely it will be in an application where a few milliseconds resolution is sufficient. The range was not fully tested on the sediments of Byfjorden. We can assume that an integration of 100 pulses will give a range similar to that of a small airgun. Deeper penetration depth can be done with longer correlation sequences. Then the measurement must be conducted with the vessel at rest. Vertical Seismic Profiling is an application of this type (MacBeth et al.,1998).

Acknowledgement

This field test was a part of the Time Coded Impulse Seismic Technique project which is supported by the Research Council of Norway. The data acquisition was conducted by Peter Skagen (Naxys), Knut Holmefjord (Naxys), Terje Ystebø (Naxys) and Ole Meyer (University of Bergen). Inge Aarseth(University of Bergen) has assisted with geological interpretations. Halfidi Halfidason(University of Bergen) has provided the Topas image.

Abbreviations

LACS	Low Level Acoustic Combustion Source
PN	Pseudo Noise
TWT	Two Way traveling Time
VSP	Vertical Seismic Profiling

References

Askeland, B., Hobæk, H., Mjelde, R. Marine seismics with a pulsed seismic combustion source and Pseudo Noise codes. Submitted to Marine Geophysical Researches march 2006.

Baeten, G., Ziolkowski, A.,1990. The Vibroseis source. Elsevier.

Chiao, R., Hao, X., 2005. Coded Excitation for Diagnostic Ultrasound: A System Developer's Perspective. IEEE Transactions on Ultrasonics, Ferroelectrics, and Frequency Control 52 (2), 160-170.

Cook, C.E., Siebert ,W.M, 1988. The Early History of Pulse Compression Radar. IEEE Transactions on Aerospace and Electronic Systems 24 (6), 825-833.

Driml, K., Reveleigh, M., Bartlett, K., 2001. Mini-SOSIE – Successful shallow 3D seismic data acquisition in an environmentally sensitive area. ASEG 15th Geophysical Conference and Exhibition, August 2001, Brisbane.

Freeman, R.L., 1994. Reference Manual for Telecommunications Engineering. Second Edition. John Wiley & Sons.

Haykin, S., 1978. Communication systems. Second edition. John Wiley & Sons.

Langhammer, J.,Landrø, M., Martin, J., Berg, E., 1995. Air-gun bubble damping by a screen. Geophysics 60 (6) 1765-1772.

Lindsey, J.P.,1991. Seismic sources I have known. Geophysics:The Leading Edge of Exploration, October, 47-48.

Mangerud, J., 1995. Western Norway. In: Andersen, B.G., Mangerud, J., Sørensen, R., Reite, A., Sveian, H., Thoresen M., Bergstrøm, B. Younger Dryas Ice-Marginal Deposits in Norway, 155-161. Quaternary International 28, 147-169.

MacBeth, C., Boyd, M., Rizer, W., Queen, J., 1998. Estimation of reservoir fracturing from marine VSP using local shear-wave conversion. Geophysical Prospecting, 46, 29-50.

Majmundar, M., Sandhu, N., Reed, J.H., 2000. Adaptive Single-User Receivers for Direct-Sequence Spread-Spectrum CDMA Systems. IEEE Transactions on vehicular technology, 49 (2) 379-389

Park, C.B., Miller, R.D., Steeples, D.W., Black, R.A., 1996. Swept impulse seismic technique (SIST). Geophysics 61 (6), 1789-1803.

Proakis, J.G., Salehi, M, 2002. Communications systems engineering. Prentice Hall.

Robinson, E.A., Treitel, S., 1980. Geophysical signal analysis. Prentice-Hall.

Tenghamn, R., Long, A., 2006. PGS shows off electrical marine vibrator to capture 'alternative' seismic source market. Eage, First Break. Volume 24, January, 33-36.

Verbeek, N.H., McGee, T.M, 1995. Characteristics of high-resolution marine reflection profiling sources. Journal of Applied Geophysics 33, 251-269.

Ziolkowski, A.M., Johnston, R.G.K., 1997. Marine seismic sources: QC wavefield computation from near-field pressure measurements. Geophysical prospecting, 45, 611-639.